Inorganica Chimica Acta 414 (2014) 63–70

Contents lists available at ScienceDirect

Inorganica Chimica Acta

journal homepage: www.elsevier.com/locate/ica

Synthesis, crystal structure and catalytic activity of a new Mo Schiff base complex with Mo histidine immobilized on Al-MCM-41 for oxidation of sulfides

Elham Zamanifar [a], Faezeh Farzaneh [a,*], Jim Simpson [b], Mahboobeh Maghami [a]

[a] Department of Chemistry, Alzahra University, PO Box 1993891176, Tehran, Iran
[b] Department of Chemistry, University of Otago, PO Box 56, Dunedin 9054, New Zealand

ARTICLE INFO

Article history:
Received 27 October 2013
Received in revised form 3 January 2014
Accepted 15 January 2014
Available online 8 February 2014

Keywords:
Dioxomolybdenum complex
Histidine
Schiff base ligand
Al-MCM-41
Sulfoxidation

ABSTRACT

A cis-dioxomolybdenum(VI) complex with Schiff base ligand derived from salicylaldehyde and L-histidine was prepared and designated as MoO_2(Sal-His). Characterization of MoO_2(Sal-His) was accomplished with elemental analysis, FT-IR, UV–Vis and TGA. X-ray crystallography studies revealed that the coordination of Mo in MoO_2(Sal-His) is a distorted octahedron formed by tetradentate histidine Schiff base ligand and two binding oxygen atoms. MoO_2(Sal-His) was used either alone or immobilized within Al-MCM-41 as sulfoxidation catalyst for a variety of sulfides with H_2O_2 as oxidant. The latter proved to be a very active and reusable heterogeneous sulfoxidation catalyst, providing 70–99% conversion and 80–95% selectivity.

1. Introduction

The coordination chemistry of molybdenum(VI) has attracted considerable interest due to the significant enzymatic role of molybdenum in biochemical reactions such as oxotransfer like nitrate reduce, xanthine oxidase/dehydrogenase, and DMSO reduce [1–3]. Molybdenum biochemical role is based on its ability to facilitate electron exchanges, forming stable complexes with oxygen-, nitrogen- and sulfur-containing ligands. This has created a tremendous impetus in the synthesis of a number of model complexes mimicking the oxotransferase molydoenzymes [3,4]. Therefore, researchers were encouraged to use molybdenum complexes as biomimetic catalysts for oxidation of aldehydes, purines and sulfides [5,6], epoxidations and hydroxylations of olefins [5–9], oxidation of alcohols [10,11] or oxygen atom transfer reactions [12].

In order to mimic biological systems, a number of dioxomolybdenum complexes have been synthesized and characterized [6,7,11,13–15]. Molybdenum Schiff base complexes continue to serve as one of the most important models of molybdoenzymes due to their preparative accessibility [5,16–23]. The activity of these complexes varies with the ligand type, coordination sites and so on.

Sulfoxidation is one of the fundamental reactions in industrial organic synthesis as sulfoxides and sulfones are biologically important compounds and have significant role in the synthesis of many organic compounds [24]. In fact, the development of novel, economical and energy efficient routes for the selective and green oxidative transformation of sulfides represents a challenge to diverse areas of contemporary chemistry. However, the homogeneous catalytic systems suffer from problems associated with the separation and recovery of the active catalyst as well as instability at high temperatures [19–23,25]. These drawbacks have so far precluded their industrial utilization. Moreover, metal contamination of products is inevitable when using homogeneous catalysts. Therefore, all strategies including catalyst reactivity, recycling, economy and environmental concerns are needed to be modified [26].

Herein, we report the synthesis and characterization of a new cis dioxomolybdenum complex with *N*-salicylidene-L-histidine Schiff base ligand, followed by immobilization within mesoporous support. The limited reports presented on molybdenum-based catalysts performing the oxidation of sulfides together with several disadvantages such as long reaction times, inconvenient conditions, expensive oxidants and low yields prompted us to investigate the catalytic activity of MoO_2(Sal-His) on sulfide oxidation.

* Corresponding author. Address: Department of Chemistry, University of Alzahra, P.O. Box 1993891176, Vanak, Tehran, Iran. Tel.: +98 21 88258977.
E-mail addresses: faezeh_farzaneh@Yahoo.com, farzaneh@alzahra.ac.ir (F. Farzaneh).

http://dx.doi.org/10.1016/j.ica.2014.01.028
0020-1693/

2. Experimental

2.1. Materials and characterization

All materials were commercial reagent grade and used without further purification. Except the *t*-butyl hydroperoxide (TBHP) purchased from Fluka, salicylaldehyde, L-histidine, sodium acetate, acetonitrile, acetone, methy phenyl sulfide, diphenyl sulfide, dimethyl sulfide, *p*-tolyl-methyl sulfide, hydrogen peroxide (30%), commercial reagent grade diethyl ether and ethanol were purchased from Merck Chemical Company.

FT-IR spectra were recorded on a Bruker Tensor 27 FT-IR spectrometer using KBr pellets over the range of 4000–400 cm^{-1}. The UV–Vis measurements were performed on a double beam UV–Vis Perkin Elmer Lambda 35 spectrophotometer. X-ray powder diffraction (XRD) data were recorded on a diffractometer type, Seifert XRD 3003 PTS, using Cu Kα_1 radiation (λ = 1.5406 Å). Single crystal measurement was performed on an Agilent SuperNova Dual single crystal diffractometer. Intensity data were collected using graphite monochromatised Mo Kα radiation (λ = 0.71073 Å). Chemical analyses of samples were determined with a Perkin-Elmer atomic absorption spectrometer (AAS). TGA/DTS was carried out by Perkin Elmer, Pyrisdiamond TG/DTA. Oxidation products were analyzed by GC and GC–MS using an Agilent 6890 Series with FID detector, HP-5, 5% phenylmethyl siloxane capillary and an Agilent 5973 Network, mass selective detector, HP-5 MS 6989 Network GC system.

2.2. Preparation of [MoO_2 (Sal-His)]

[MoO_2(Sal-His)] was prepared using the reported procedure [23]. Salicylaldehyde (10 mmol in 20 mL ethanol) was introduced into the histidine solution (10 mmol in 20 mL water). Upon addition of an aqueous sodium acetate solution (0.02 mol in 10 mL water), the color was changed to deep yellow. $MoO_2(acac)_2$ (8.5 mmol, prepared according to the literature method [27] in 10 mL ethanol) was then added and the mixture was heated at reflux for 5 h while stirring. The yellow resultant solid was filtered, washed with water, acetone, and diethyl ether, and dried in air at room temperature. X-ray quality crystals of the complex [MoO_2(Sal-His)] was obtained by slow diffusion of diethyl ether into the saturated [MoO_2(Sal-His)]solution in dimethylformamide.

Anal. Calc. for $C_{13}H_{11}N_3O_5Mo$ (M = 385 g mol^{-1}): Mo, 25.00; C, 40.62; H, 2.60; N, 10.94. Found: Mo, 25.19; C, 40.67; H, 2.61; N, 10.93%. FT-IR (KBr pellet) cm^{-1}: 1631 (C=N), 1603, 1347 (COO^-), 1556 (C=C), 1315 (O–Ph), 910, 930 (cis-MoO_2), which are consistent spectral bands with those reported previously [28,29]. UV–Vis: λ_{max} at 270, 285, 346, 414 nm [28,30]. ^{1}H NMR (DMSO-d_6) δ 3.19–3.24 (m) (β-CH_2), 7.11 (m) (imidazol-5-H), 7.56–7.69 (m) (Ar–H), 8.37 (d) (imidazol-2-H), 9.00 (s) (CH=N), 12.82 (s) broad (imidazol N–H). ^{13}C NMR (DMSO-d_6) δ 116.0 (imidazole-C_2), 118.8 (Ar), 122.7 (Ar), 123.0 (Ar), 133.1 (A), 135.1 (imidazole-C_5), 136.8 (Ar), 162.5 (CH=N), 165.4 (Ph), 174.6 (C=O) [28].

2.3. Preparation of catalyst

Al-MCM-41 (1 g), prepared according to the previously reported method [31], was added to the complex (0.26 mmol in 20 mL ethanol). The mixture was heated at reflux for 8 h while stirring. The resultant MoO_2(Sal-His)/Al-MCM-41 solid was then filtered, washed with hot ethanol and dried in air at room temperature. The molybdenum percentage was determined by AAS to be 3.36%.

2.4. General procedure for the oxidation of sulfides

A mixture of Mo-catalyst (40 mg) and substrate (20 mmol in 5 cc acetonitrile) was slowly stirred in a round bottom flask. H_2O_2 (30% aqueous solution, 20 mmol) was then added and the mixture stirred for a few minutes at room temperature. After filtration and washing the solid with fresh acetonitrile, the filtrate was subjected to GC and GC Mass analysis.

2.5. X-ray crystallography

Yellow crystals of [MoO_2(Sal-His], 1, were grown by diffusion of ether into a DMF complex solution. X-ray data for **1** was collected on an Agilent SuperNova Dual single crystal diffractometer. Mo Kα radiation (λ = 0.71073 Å) was used for the collection which was controlled by CRYSALISPRO [32] with data collected at 100(2) K. Data was corrected for Lorentz and polarization effects using multi-scan absorption corrections were applied using CRYSALISPRO [32]. The structure was solved by direct methods (SHELXS-97) [33] and refined using full-matrix least-squares procedures (SHELXL-97 [33] and TITAN2000) [34]. All non-hydrogen atoms were refined anisotropically and those hydrogen atoms bound to carbon were placed in the calculated positions, and their thermal parameters were refined isotropically with *U*eq = 1.2 *U*eq(C). The hydrogen atom bound to N1 was located in a difference Fourier map and its coordinates were refined with *U*eq = 1.2 *U*eq (N). All molecular plots and packing diagrams were drawn using MERCURY [35] and additional metrical data was calculated using PLATON [36]. Crystallographic data and details of collected data and structure refinement are listed in Table 1. Selected bond lengths and angles are shown in Table 2.

3. Results and discussion

Salicylaldehyde and L-histidine were treated with $MoO_2(acac)_2$ in ethanol and water. As seen in Scheme 1, the initially generated *N*-salicylidene-L-histidine Schiff base ligand from condensation of salicylaldehyde and L-histidine undergoes complexation with

Table 1
Selected crystallographic data and details for the structure refinement of [MoO2(Sal-His].

Empirical formula	$C_{13}H_{11}MoN_3O_5$
Formula weight	385.19
Crystal system; space group	monoclinic, *P* 21/*n*
a (Å)	7.43173(17)
b (Å)	10.7623(2)
c (Å)	17.3644(4)
β (°)	101.948(2)
V (Å^3)	1358.77(5)
Z	4
Absorption coefficient (mm^{-1})	0.994
D_{calc} (Mg m^{-3})	1.883
R_{int}	0.0311
Crystal size (mm^3)	0.2 × 0.2 × 0.2
θ Range for collection (°)	3.3680–29.3850
Index ranges	$-10 \leqslant h \leqslant 10$ $-13 \leqslant k \leqslant 14$ $-23 \leqslant l \leqslant 23$
Reflections collected	15 698
Independent reflections	3465
Independent reflections [$I > 2\sigma(I)$]	3132
Maximum and minimum transmission	1.00–0.87500
Data/restraints/parameters	3465/0/202
Final *R* indices [$I > 2\sigma$ (*I*)]	R_1 = 0.0285 wR_2 = 0.0572
R indices (all data)	R_1 = 0.0242 wR_2 = 0.0545

Table 2
Selected bond lengths (Å) and angles (°) for [MoO2(Sal-His].

Bond lengths (Å)	
Mo(1)–O(1)	1.7012(13)
Mo(1)–O(2)	1.7090(14)
Mo(1)–O(12)	1.9376(13)
Mo(1)–O(82)	2.0450(13)
Mo(1)–N(4)	2.2287(15)
Mo(1)–N(3)	2.3694(15)
Bond angles (°)	
O(1)–Mo(1)–O(2)	107.26(7)
O(1)–Mo(1)–O(12)	96.60(6)
O(2)–Mo(1)–O(12)	99.90(6)
O(1)–Mo(1)–O(82)	93.71(6)
O(2)–Mo(1)–O(82)	100.25(6)
O(12)–Mo(1)–O(82)	153.48(5)
O(1)–Mo(1)–N(4)	95.02(6)
O(2)–Mo(1)–N(4)	157.35(6)
O(12)–Mo(1)–N(4)	81.11(6)
O(82)–Mo(1)–N(4)	73.68(5)
O(1)–Mo(1)–N(3)	167.49(6)
O(2)–Mo(1)–N(3)	84.18(6)
O(12)–Mo(1)–N(3)	86.12(6)
O(82)–Mo(1)–N(3)	78.96(5)

$MoO_2(acac)_2$, affording [MoO_2(Sal-His)]. The ligand acts as a tetradental ONON donor towards the MoO_2^{2+} core.

3.1. Crystal structure determination

An ORTEP view (50% thermal ellipsoids) of [MoO_2(Sal-His] is shown in Fig. 1. The Mo atom in the complex [MoO_2(Sal-His] adopts a severely distorted octahedral 6-coordinated geometry Fig. S1 (see Supplementary) with the Mo=O1 and Mo=O2 distances of 1.7012 (13) and 1.7090 (14) Å respectively, typical of a double bond. Bond angles in the octahedron vary from 73.28(5)° to 107.26(7)° for *cis*-substitued and 167.49(6)° to 153.48(5)° for *trans* substituted, indicating the significance of distortion degree in the octahedron.

The aminoacid–salicylaldehyde ligand coordinates to the MoO_2^{2+} moiety as a tetradentate [N3,O12,N4,O82] chelating ligand via the deprotonated carboxylic acid and phenoxy oxygen atoms, together with the two imine N atoms. In the process, two five membered and one six-membered chelate rings are formed. Chelation of this type to a Mo atom has no precedent in the Cambridge Structural Database [37] although there are several instances of an imidazole molecule binding through its imine N atom to an MoO_2^{2+} unit which in term is coordinated to a tridentate O,N,O ligand [38]. There is a distinct trend in Mo–O bond lengths in the complex with Mo=O1/2 (terminal) ≪ Mo–O12 (phenoxyl) < Mo–O82 (carboxyl). Also the *trans* influence ensures that both Mo–N distances *trans* to the M=O bonds are significantly extended (Table 2).

In the crystal structure, N1–H1N···O82^{i} hydrogen bonds bolstered by C2–H2···O81 contact link molecules into zigzag chains along *b* (Fig. 2).

Several other C–H···O contacts (Table 3), and a π···π stacking interaction between the benzene rings of adjacent molecules with a centroid···centroid distance of 3.5791(12) Å further stabilize the structure stacking molecules along the crystallographic *b* axis Fig. S2 (see Supplementary).

3.2. NMR studies

The coordinating modes of the ligand were confirmed by comparison of ^{1}H NMR (DMSO-d_6) spectrum of the ligand with that of complex. A significant downfield shift ($\Delta\delta$ = 0.85 ppm) of the

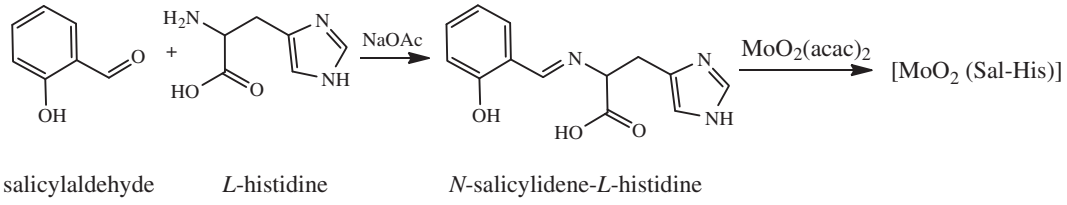

Scheme 1. Preparation of MoO2(Sal-His).

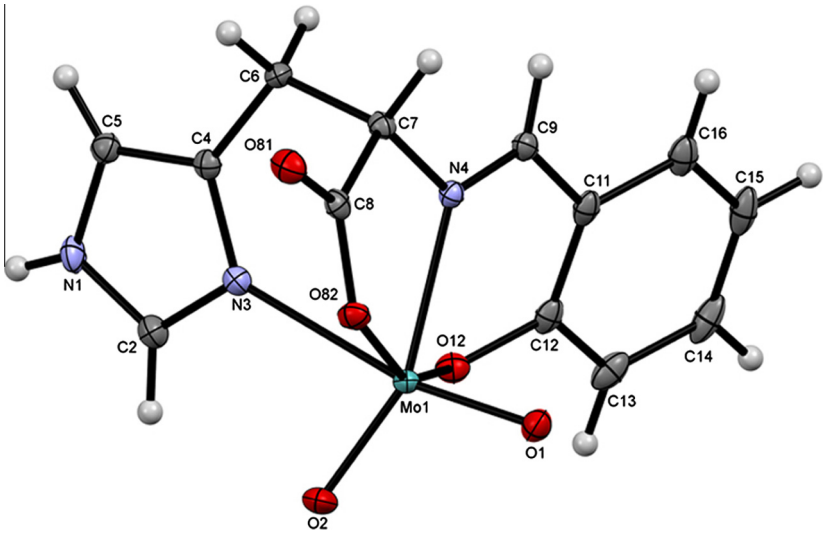

Fig. 1. The structure of **1** showing the atom numbering and with ellipsoids drawn at the 50% probability level.

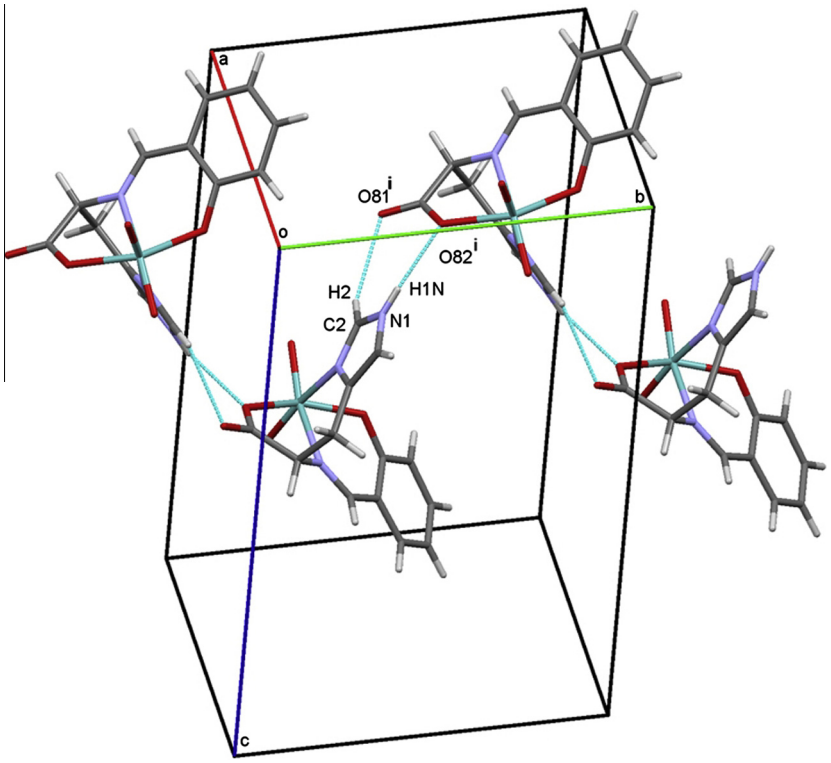

Fig. 2. Zig-zag chains of molecules of **1** with hydrogen bonds drawn as dashed lines. Symmetry operation i = −1 + *x*,*y*,*z*.

Table 3
Hydrogen bond distances (Å), angles (°) for 1.

D–H···A	D–H	H···A	D···A	⟨D–H···A
N1–H1N···O2i	0.79(3)	2.23(3)	2.985(2)	160(2)
C2–H2···O81i	0.95	2.55	3.140(2)	121
C6–H6B···O2ii	0.99	2.43	3.102(2)	125
C7–H7···O2ii	1.00	2.60	3.193(2)	118
C9–H9···O2ii	0.95	2.53	3.349(2)	145

Symmetry operations: i = −1 + *x*,*y*,*z*; ii = −1/2 − *x*,1/2 + *y*,1/2 − *z*.

complex azomethine (—CH═N—) proton relative to the corresponding ligand demonstrates the coordination of azomethine nitrogen atom. Aromatic protons appear in the expected regions in the spectra of the ligand as well as of the complex with minor variation in their positions. The signal appears at low field (δ = 12.82 ppm) is assigned to the imidazole NH. The ^{13}C NMR spectrum shows thirteen distinct carbon signals consistent with the single crystal structure Fig. S3 (see Supplementary).

3.3. FTIR studies

The FT-IR spectra of Sal-His and MoO_2(sal-his) are shown in Fig. 3A and B, respectively. As seen in Fig. 3A, the bands appear at 1603 and 1347 cm^{-1} are due to the asymmetric COO^- and symmetric COO^- vibrations. The C═N stretching of the complex appearing at 1631 cm^{-1} shows a slightly lower frequency in comparison to the corresponding vibration in the spectrum of the free ligand (1635 cm^{-1}). Recall that the involvement of the imine lone pairs in bonding to metal ion shifts the C═N to lower frequency. The rather large difference between asymmetrical and symmetrical COO^- frequencies indicates a monodentate coordination of this group [39]. The O–H stretching frequency of the free ligand displaying at 3425 cm^{-1} disappeared after complexation due to the deprotonation of COO–H group and formation of Mo–O bond.

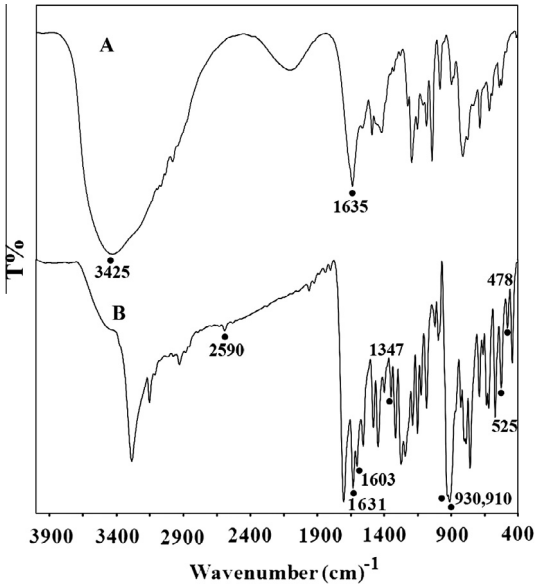

Fig. 3. FT-IR spectra of (A) Ligand schiff-base N-salicyliden-L-histidine (Sal-His), (B) MoO2(Sal-His).

Strong band appearing at 1315 cm^{-1} is perhaps due to C–O vibration. The carboxylic acid group of the Schiff base ligand was deprotonated because the solution was kept alkaline upon addition of sodium acetate in the preparation procedure. For this and what was reported previously for vanadium complexes [29,30], the coordination of the carboxylate oxygen to the metal center is concluded. The weak band displaying at 2590 cm^{-1} in the complex spectrum due to imidazole NH group indicates that it has not undergone deprotonation. Due to the rather harsh synthetic conditions of temperature and alkalinity, the dianionic ligand has

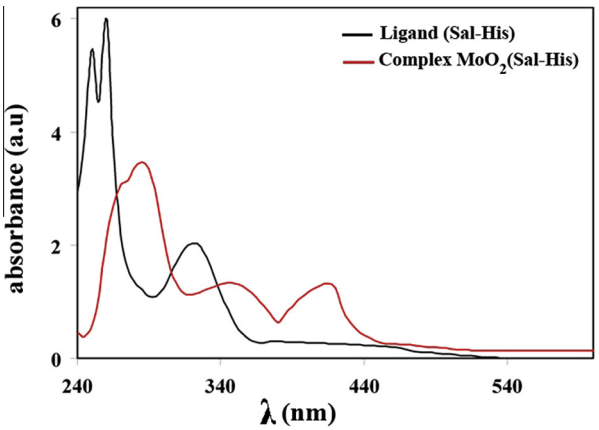

Fig. 4. Electronic spectra of [MoO2(Sal-His)] in acetonitrile.

undergone deprotanation at carboxylic acid and phenol groups on complexation, Observation of two bands at 930 and 910 cm^{-1} regions are due to the Mo=O vibrations [40]. The two bands displaying at 525 cm^{-1} and 478 cm^{-1} of the low frequency region are attributed to the Mo–O and Mo–N, generated by Mo complexation to the phenol O and azomethine N atoms, respectively [41].

Notably, the consistency of the elemental analysis results of the complex with molecular structure obtained from X-ray crystallography clearly indicates that no solvent (H_2O or EtOH) has been involved in bonding to the metal center. On the other hand, the involvement of imidazole group of the aminoacid in coordination is consistent with X-ray single crystal structure.

3.4. UV studies

Investigation of the electronic spectra of Schiff base ligand exhibits three main peaks at 250 ($\varepsilon = 5.45 \times 10^3\ M^{-1}\ cm^{-1}$), 260 ($\varepsilon = 6.00 \times 10^3\ M^{-1}\ cm^{-1}$) and 321 nm ($\varepsilon = 2.03 \times 10^3\ M^{-1}\ cm^{-1}$) (Fig. 4). The first and second peaks are attributed to the benzene $\pi \rightarrow \pi^*$ and imine $\pi \rightarrow \pi^*$ transitions, respectively. These bands were slightly affected by chelation and shifted to longer wavelength 270 and 285 nm with relatively decrease in their intensities. The third band is assigned to the $n \rightarrow \pi^*$ transition. This band is shifted to longer wavelength at 347 nm together with increasing in intensity. This shift may be attributed to the nitrogen atom donation lone pairs of the Schiff base to the metal ion (N → M) [42]. The absorption maximum appearing at 414 nm could be assigned to ligand to metal charge transfer (LMCT) Mo ($d\pi$) → O (π). Recall that this is in the range usually observed for MoO complexes [43].

3.5. TGA/DSC

A deeper insight into the structure of complex was undertaken using thermogravimetry (TG) and differential scanning calorimetry techniques (Fig. 5). The [Mo(O_2)($C_{13}H_{11}N_3O_3$)] complex with 385 M mass showed a thermal stability from room temperature up to 300 °C. Observing two weight looses at 317 and 450 °C are due to the decomposition of organic ligand (obs.: 62%, calcd.: 62.53%) and ended with molybdenum oxide MoO_3 (obs.: 38%, calcd.:37.47%).

3.6. MoO_2(Sal-His)/Al-MCM-41 characterization

The X-ray powder diffraction pattern of calcined Al-MCM-41 and MoO_2(Sal-His)/Al-MCM-41 are shown in Fig. S4 (see Supplementary). Whereas the former is consistent with those reported before [31] and can be indexed on a hexagonal lattice, the latter displays a decrease in the peak intensity in comparison to that of calcined Al-MCM-41. Such changes clearly indicate that Mo complex has been immobilized on Al-MCM-41. Observation of the shift in reflection to lower angle (or higher *d*-value) also indicates expansion in unit cell parameter due to the immobilization of the complex within Al-MCM-41 pores (Table 4).

The low temperature N_2 adsorption–desorption analyses was performed in order to investigate the textural properties such as surface area, pore volume and pore diameter of the resultant materials after immobilization of dioxo molybdenum Schiff base complex. Observation of type IV isotherms [44] in the MoO_2 (Sal-His)/Al-MCM-41 N_2 adsorption–desorption (Fig. S5 (see Supplementary) indicates that the adsorption takes place as a thin layer on the walls at low relative pressures, P/P0 (monolayer coverage). In addition, the inflection heights are smaller than those of Al-MCM-41 Fig. S5 (see Supplementary). This phenomenon is attributed to the reduced pore volume from 1.074 to 0.8416 $cm^3\ g^{-1}$, which reflects the decrease in surface area (Table 4), perhaps due to the inclusion of MoO_2(Sal-His) within the Al-MCM-41. Despite the decrease in the specific surface area of the prepared catalyst,

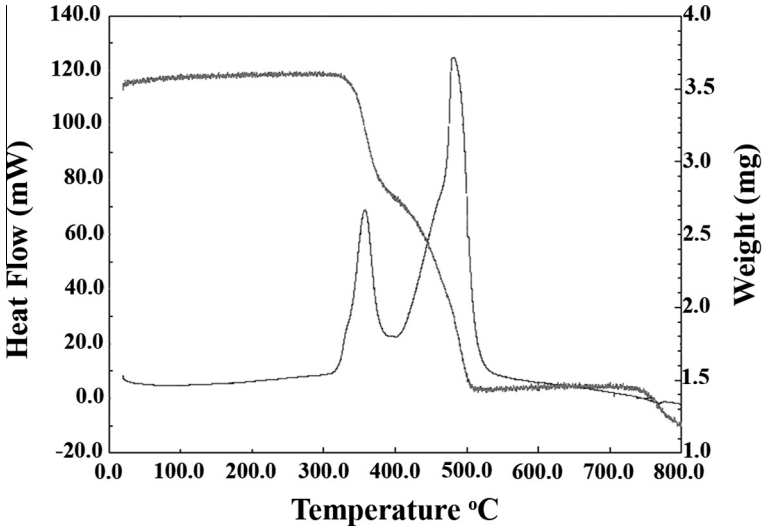

Fig. 5. TGA and DSC curves of the MoO2(Sal-His) complex.

Table 4
Sample texture parameters obtained from XRD and nitrogen sorption studies.

Material	XRD d value (Å)	Lattice parameter (Å)	BET[a] (m^2 g^{-1})	Pore volume (cm3 g-1)	Average pore diameter (Å)
Al-MCM-41	32.5	37.53	1455	1.074	20.72
MoO2(Sal-His)/Al-MCM-41	33.90	39.14	1030	0.8416	19.12

[a] Specific surface area.

the remaining space in pores is still so large that many of the organic substrates can enter into the channels.

The FT-IR spectra of MoO_2(Sal-His)/Al-MCM-41, Al-MCM-41 and the drift of FTIR or the difference between the immobilized complex on Al-MCM-41 and Al-MCM-41 are shown in Fig. 6A–C, respectively. The broad bands appearing at 3424 to 3445 cm^{-1} may be attributed to the surface silanol and –OH groups of the adsorbed water, respectively. After immobilization of the complex within Al-MCM-41, some weak peaks appearing in the region of 2900 to 3160 cm^{-1} due to the C–H and N–H vibrations. Whereas the band displaying at 1200 to 1080 cm^{-1} belong to the asymmetrical stretching vibrations of Si–O–Si bridges, those displaing at 961 to 803 cm^{-1} arise from Si–O–Al stretching vibrations. However, observing a band at 930 cm^{-1} is due to the MoO_2 stretching vibration. The stretching frequency of the C=N group of the immobilized molybdenum complex within the Al-MCM-41 appears at 1632 cm^{-1}. The subtracted spectrum of the immobilized complex within Al-MCM-41 from that of Al-MCM-41 reveals a band at 1632 and two medium intensity bands at 909 and 937 cm^{-1} that are assigned to C=N and Mo=O stretchings, respectively. The asymmetrical and symmetrical COO– and C–O vibration bands are also observed at 1334 and 1594 and 1312 cm^{-1}, respectively. These observations confirm the presence of the immobilized complex within Al-MCM-41.

TG/DTA patterns of MoO_2(Sal-His)/Al-MCM-41 are shown in Fig. S6 (see Supplementary). The weight loss of the complex immobilized within nanoreactors of Al-MCM-41 take places at two steps. The first weight loss of 5.5% is observed below 350 °C, corresponding to the evaporation of water and organic solvent (ethanol). The second weight loss observed at about 400–700 °C is due to decomposition of the organic ligand, consistent with DTA result.

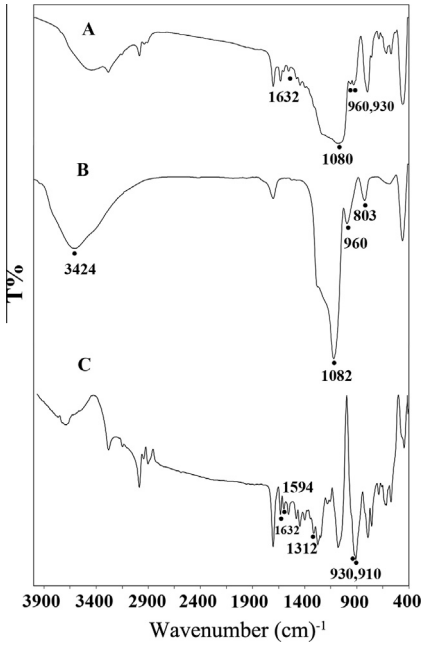

Fig. 6. FT-IR spectra of (A) MoO2(Sal-His)/Al-MCM-41, (B) Al-MCM-41 and (C) the spectrum of the difference of MoO2(Sal-His)/Al-MCM-41 and Al-MCM-41.

3.7. Catalytic studies

3.7.1. Catalytic activity of MoO_2(Sal-His)/Al-MCM-41 in the oxidation of sulfides

To find optimum reaction conditions, we initially investigated the influence of factors such as oxidant, amount of catalyst and reaction time on the conversion and selectivity of sulfide oxidations. The oxidation of phenyl methyl sulfide was carried out as the model reaction in the presence of H_2O_2 and TBHP at room temperature in acetonitrile as solvent. It was found that H_2O_2 is a better oxidizing agent due to higher sulfide conversion.To optimize the amount of catalyst, sulfoxidation of phenyl methyl sulfide was carried out within 60 min using 30, 40 and 50 mg of catalyst. As indicated in Table 5 and 40 mg of catalyst proved to be sufficient for 97% conversion of methyl phenyl sulfide with 94% percent selectivity toward the formation of methyl phenyl sulfoxide as the major product. Whereas increasing of the catalyst to 50 mg partially increased the conversion, but resulted in the corresponding sulfoxide in lower yield (Table 5).

To obtain the best reaction time, the oxidation reactions were carried out within different times (Fig. 7). Whereas 97% of the methyl phenyl sulfide was converted resulting in 94% sulfoxide during 60 min, no considerable oxidation occurred during the next 30 min.

Encouraged by this result, the new method was applied to a variety of sulfides. We have included the effect of Al-MCM-41 void of complex as catalyst and those oxidation results obtained using $MoO_2(acac)_2$/Al-MCM-41 and blank reaction in Table 6 in order to make the comparison more convenient. As seen in Table 6, all substrates were converted into the corresponding sulfoxides with moderate to high yields and excellent selectivities under mild conditions. Notably, sulfoxidation of dialkyl sulfide proceeded to almost completion within 60 min (entry 1, Table 6). Whereas replacement of an alkyl with a phenyl group resulted in lower yield (entries 2 and 5, Table 6), sulfoxidation of diphenyl sulfides had to be carried out under reflux condition (entries 3 and 4, Table 6).

Compared to using MoO_2(Sal-His) as a homogeneous catalyst (entry 7d, Table 6), Al-MCM-41 void of complex (entry 7e, Table 6) and $MoO_2(acac)_2$/Al-MCM-41 (entry 7f, Table 6), oxidation of methyl phenyl sulfide using the heterogeneous MoO_2(Sal-His)/Al-MCM-41 catalysis system afforded the methyl phenyl sulfoxide in 97% yield (entry 5, Table 6). These results clearly indicate the

Table 5
The influence of amount Mo-catalyst on the oxidation of methyl phenyl sulfide.

Entry	Catalyst amount (mg)	Conversion (%)	Selectivity (%)		TON[a]
			Sulfoxide	Sulfone	
1	30	86	97	3	1638
2	40	97	94	6	1386
3	50	98	90	10	1120

Reaction conditions: substrate (20 mmol), oxidant (H2O2, 30%, 20 mmol), solvent (acetonitrile, 5 mL), Time (60 min), room temperature.
[a] TON is the mmol of product to the mmol molybdenum present in catalyst.

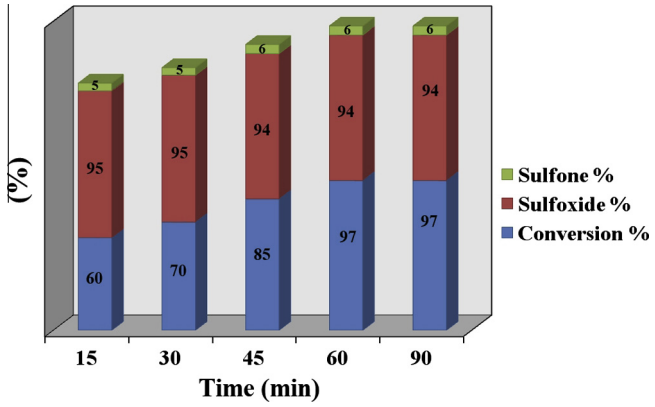

Fig. 7. Conversion of methyl phenyl sulfide at different times in the presence of MoO2(Sal-His)/Al-MCM-41 catalyst.

Table 6
Oxidation of sulfides using MoO2(Sal-His)/Al-MCM-41 as catalyst.

Entry	Substrate	Conversion (%)	Selectivity (%)		TON[a]
			Sulfoxide	Sulfone	
1	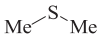	99	90	10	1414
2	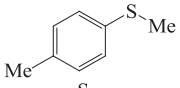	98	95	5	1400
3	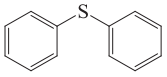	70	80	20	1000
4	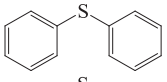	90[b]	86	14	1286
5	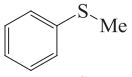	97	94	6	1386
6	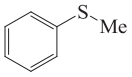	95[c]	94	6	1357
7	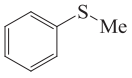	80[d,e,f,g]	85	15	1143

Reaction conditions: catalyst (40 mg), substrate (20 mmol), oxidant (H_2O_2, 30%, 20 mmol), solvent (acetonitrile, 5 mL, Time (60 min), room temperature.
[a] TON is the mmol of product to mmol molybdenum present in catalysts.
[b] Under reflux conditions.
[c] Reaction was carried out in the presence of recovered catalyst.
[d] Reaction was carried out in the presence of MoO_2(Sal-His) as a homogeneous catalyst.
[e] 15% Conversion was obtained when reaction was carried out in the presence of Al-MCM-41 void of complex.
[f] 70% Conversion was obtained when reaction was carried out in the presence of $MoO_2(acac)_2$/Al-MCM-41.
[g] 10% Conversion was obtained in blank reaction.

key effect of the complex immobilized within the Al-MCM-41 in enhancing the sulfoxidation percentage yield as well as the selectivity toward the desired product.

The recyclability of the heterogenised molybdenum catalysis system for the oxidation of the methyl phenyl sulfide was investigated by recovering the catalyst, washing, drying at 100 °C to remove the adsorbed solvent and reusing it in another sulfoxidation reaction under similar conditions (entry 6, Table 6). Notably, 2% loss in sulfide conversion with similar selectivity was observed. As such, it can be concluded that the active species has been remained almost intact within the Al-MCM-41 support. Moreover, detecting no molybdenum in the filtrate using the ICP-AAS method not only rules out any complex desorption, but also support the heterogeneity of our catalysis system.

Compared to the catalytic activity of the reported homogeneous catalysis systems [13,22,45] the heterogeneity and stability of MoO_2(Sal-His)/Al-MCM-4 catalyst is notable. In fact, utilization of solid support offers the advantages of easy catalyst separation and possible catalyst recycling. Particularly significant in this case is the high activity and selectivity of our catalysis system. In addition, the provided method is an interesting approach to the immobilizing biomimetic Mo complex in order to investigate the oxidation catalytic type reactions.

4. Conclusions

An expedient procedure was provided for the synthesis of dioxomolybdenum(VI) with tetradental *N*-salicylidene-L-histidin Schiff base complex. In fact, the coordination of the aminoacid as histidine is also interesting regarding some enzymatic reactions such as nitrogenase. The molybdenum complex [MoO_2(Sal-His)] was then immobilized within Al-MCM-41 nanoreactors. The prepared heterogeneous molybdenum was found to successfully catalyze the oxidation of sulfides. Compared to using MoO_2(Sal-His) alone as a homogeneous catalyst, immobilization within Al-MCM-41 proved to enhances the sulfoxidation catalytic activity. The reusability of the recovered catalyst with rather similar catalytic activity along with detecting no molybdenum desorption into the filtrate indicates the heterogeneous character of the examined catalysis system. Overall, utilization of an easily prepared heterogeneous catalyst and using environmentally benign oxidants together with mild reaction conditions and obtaining moderate to high yields of the desired product with excellent selectivity, short reaction time, and reusability of the catalyst with no marked drop in conversion make the present protocol a green and efficient alternative for the synthesis of commercially important sulfoxides.

Acknowledgement

The financial support from the University of Alzahra is gratefully acknowledged.

Appendix A. Supplementary material

Supplementary data associated with this article can be found, in the online version, at http://dx.doi.org/10.1016/j.ica.2014.01.028.

References

[1] A. Majumdar, S. Sarkar, Coord. Chem. Rev. 255 (2011) 1039.
[2] S. Metza, W. Thiel, Coord. Chem. Rev. 255 (2011) 1085.
[3] R.H. Holm, E.I. Solomon, A. Majumdara, A. Tenderholt, Coord. Chem. Rev. 255 (2011) 993.
[4] R.H. Holm, Chem. Rev. 87 (1987) 1401.
[5] R.D. Chakravarthy, D.K. Chand, J. Chem. Sci. 123 (2011) 187.
[6] J.M. Bregeauit, Dalton Trans. (2003) 3289.
[7] A.A. Valente, J. Moreira, A.D. Lopes, M. Pillinger, C.D. Nunes, C.C. Romao, F.E. Kuhnd, I.S. Goncalves, New J. Chem. 28 (2004) 308.
[8] S.N. Rao, K.N. Munshi, N.N. Rao, J. Mol. Catal. A: Chem. 156 (2000) 205.
[9] M. Bagherzadeh, L. Tahsini, R. Latifi, L.K. Woo, Inorg. Chim. Acta 362 (2009) 3698.
[10] C.Y. Lorber, S.P. Smidt, J.A. Osborn, Eur. J. Inorg. Chem. (2000) 655.
[11] Y.L. Wong, A.R. Cowley, J.R. Dilworth, Inorg. Chim. Acta 357 (2004) 4358.
[12] R.H. Holm, Coord. Chem. Rev. 100 (1990) 183.
[13] M. Bagherzadeh, L. Tahsini, R. Latifi, A. Ellern, L.K. Woo, Inorg. Chim. Acta 361 (2008) 2019.
[14] A.J. Burke, Coord. Chem. Rev. 252 (2008) 170.
[15] J. Hakala, R. Sillanpää, A. Lehtonen, Inorg. Chem. Commun. 21 (2012) 21.
[16] A. Syamsl, M.R. Maurya, Coord. Chem. Rev. 95 (1989) 183.
[17] Y. Sui, X. Zenga, X. Fang, X. Fub, Y. Xiao, L. Chend, M. Li, S. Chenga, J. Mol. Catal. A: Chem. 270 (2007) 61.
[18] S.N. Rao, N. Kathale, N.N. Rao, K.N. Munshi, Inorg. Chim. Acta 360 (2007) 4010.
[19] M. Mancka, Inorg. Chem. Commun. 10 (2007) 677.
[20] I. Sheikhshoaie, A. Rezaefard, N. Monadi, S. Kaafi, Polyhedron 28 (2009) 733.
[21] R.D. Chakravarthy, K. Suresh, V. Ramkumar, D.K. Chand, Inorg. Chim. Acta 376 (2011) 57.

[22] M. Bagherzadeh, M. Amini, H. Parastar, M. Jalali-Heravi, A. Ellern, L. Keith Woo, Inorg. Chem. Commun. 20 (2012) 86.
[23] N.Y. Jin, W.H. Li, Synth. React. Inorg. Met. -Org. Nano-Met. Chem. 42 (2012) 1167.
[24] A.G. Renwick, in: L.A. De Damani (Ed.), Sulfur-Containing and Related Organic Compounds, Vol. 1, Part B, Ellis Horwood, Chichester, UK, 1989, p. 133.
[25] C.A. Gamelas, T. Lourenço, A.P. da Costa, A.L. Simplício, B. Royo, C.C. Romão, Tetrahedron Lett. 49 (2008) 4708.
[26] R.K. Sharma, A. Pandey, S. Gulati, Polyhedron 45 (2012) 86.
[27] G.J. Chen, J.W. Mc, Inorg. Chem. 15 (1976) 2612.
[28] L. Casella, M. Gullotti, A. Pintar, Inorg. Chim. Acta 144 (1988) 89.
[29] J. Costa Pessoa, I. Cavaco, I. Correia, M.T. Duarte, R.D. Gillard, R.T. Henriques, F.J. Higes, C. Maderia, I. Tomaz, Inorg. Chim. Acta. 293 (1999) 1.
[30] R. Ando, H. Inden, M. Sugino, H. Ono, D. Sakaeda, T. Yagyu, M. Maeda, Inorg. Chim. Acta 357 (2004) 1337.
[31] M.A. Zanjanchi, Sh. Asgari, Solid State Ionics 171 (2004) 277.
[32] Agilent Technologies Ltd, CRYSALISPRO, Agilent Technologies Ltd, Yarnton, England, 2013.
[33] G.M. Sheldrick, Acta Crystallogr., Sect. A 64 (2008) 112.
[34] K.A. Hunter, J. Simpson, TITAN2000, University of Otago, New Zealand, 1999.
[35] C.F. Macrae, I.J. Bruno, J.A. Chisholm, P.R. Edgington, P. McCabe, E. Pidcock, L. Rodriguez-Monge, R. Taylor, J. van de Stree, P.A. Wood, J. Appl. Crystallogr. 41 (2008) 466.
[36] A.L. Spek, Acta Crystallogr., Sect. D 65 (2009) 148.
[37] F.H. Allen, Acta Crystallogr., Sect. B. 58 (2002) 380.
[38] (a) S. Pasayat, S.P. Dash, Polyhedron 38 (2012) 198;
(b) N.K. Ngan, K.M. Lo, C.S.R. Wong, Polyhedron 30 (2011) 2922;
(c) C. Zhang, G. Rheinwald, V. Lozan, B. Wu, P.-G. Lassahn, H. Lang, C. Janiak, Z. Anorg. Allg. Chem. 628 (2002) 1259;
(d) R. Dinda, P. Sengupta, S. Ghosh, H. Mayer-Figge, W.S. Sheldrick, J. Chem. Soc., Dalton Trans. (2002) 4434;
(e) K. Uzarevic, M. Rubcic, M. Radic, A. Puskaric, M. Cindric, CrystEngComm 13 (2011) 4314;
(f) R. Dinda, P. Sengupta, S. Ghosh, W.S. Sheldrick, Eur. J. Inorg. Chem. (2003) 363;
(g) P.F. Wu, D.S. Li, X.G. Meng, X.L. Zhong, C. Jiang, Y.L. Zhu, Y.G. Wei, Acta Crystallogr., Sect. E 61 (2005) m1553;
(h) L.T.J. Delbaere, C.K. Prout, J. Chem. Soc. D (1971) 162;
(i) B. Spivack, Z. Dori, J. Chem. Soc., Dalton Trans. (1975) 1077.
[39] K. Nakamoto, Infrared and Raman Spectra of Inorganic Compounds, fifth ed., 1997, p. 271.
[40] O.A. Rajan, A. Chakravorty, Inorg. Chem. 20 (1981) 660.
[41] G. Wang, J.C. Chang, Synth. React. Inorg. Met. -Org. Chem. 24 (1994) 1091.
[42] B.N. Ghose, K.M. Lasisi, Synth. React. Inorg. Met. -Org. Chem. 16 (1986) 1121.
[43] N. Sumita Rao, M.N. Jaiswal, D.D. Mishra, R.C. Maurya, Polyhedron 12 (1993) 2045.
[44] J. Lynch, Physico-Chemical Analysis of Industrial Catalysts, Technip ed, Paris, 2001.
[45] S. Colonna, A. Manfredi, M. Spadoni, L. Casella, M. Gullotti, J. Chem. Soc., Perkin Trans. 1 (1987) 71.